Acta Pharm. **74** (2024) 461–478
https://doi.org/10.2478/acph-2024-0025

Original research paper

Trifarotene alleviates skin photoaging injury by inhibition of JNK/c-Jun/MMPs

XUAN FEI[1,a]
LELE ZIXIN YANG[2,a]
JINGJING ZHANG[1]
XIANG LI[1]
MENGTIAN PAN[1]
GUANGCHEN XU[1]
CUIXIA ZHANG[3]
FEI LIU[3,*]
WEIRONG FANG[1,*]

[1] *Department of Physiology School of Basic Medicine and Clinical Pharmacy, China Pharmaceutical University Nanjing 210009, P.R. China*

[2] *Sidney Kimmel Medical College, Philadelphia, USA*

[3] *Nanjing Minova Pharmaceuticals, Nanjing 210000, P.R. China*

Accepted June 7, 2024
Published online June 7, 2024

ABSTRACT

Long-term exposure to ultraviolet (UV) radiation induces skin photoaging, which manifests as oxidative stress, inflammation, and collagen degradation. Multiple approaches (topical or systemic retinoids, antioxidants, alpha-hydroxy acids, laser, surgery) are used in the treatment of photoaged skin, and the use of topical retinoids is currently a primary clinical treatment. Previous studies revealed that retinoic acid promotes keratinocyte proliferation and reduces melanin deposition and matrix metalloproteinase (MMP) secretion; it also causes potential allergic and inflammatory damage to the skin. This study aimed to investigate the therapeutic effects and mechanisms of trifarotene, a functional retinoic acid analog, on UV-irradiated photoaging ICR and BALB/c nude mice and UVB photodamaged human epidermal keratinocyte (HaCaT) cells by examining indicators such as collagen, oxidoreductase, and inflammatory factor presence through histochemical staining, Western blot, and ELISA. Results suggested that trifarotene significantly reduced UV-induced photoaging in mouse skin tissue, potentially by reducing oxidative stress damage and inflammatory factor release, and inhibiting melanin deposition and collagen degradation by downregulating MMP expression. Concentrations of malondialdehyde, tyrosinase, interleukin-6, interleukin-12, and tumor necrosis factor-alpha in photoaged skin decreased, while SOD content in photodamaged HaCaT cells significantly increased. Trifarotene (3.3 μmol L^{-1}) inhibited phosphorylated JNK and c-Jun expression both independently and collaboratively with the JNK activator anisomycin, demonstrating that trifarotene mitigates UV-induced collagen degradation and apoptosis through inhibition of the JNK/c-Jun/MMPs signaling pathway.

Keywords: trifarotene, skin photoaging, UV, matrix metalloproteinases, inflammatory factors

INTRODUCTION

The skin is the first physiological barrier of the body and protects tissues and organs from damage caused by external factors such as ultraviolet radiation, which causes photoaging in the long term (1, 2). Characteristic clinical manifestations of skin photoaging are

[a] These authors contributed equally to this work.
* Correspondence; e-mails: liufei@mnvpharma.com; weirongfang@163.com

mainly dry, rough skin, deep wrinkles, melanin deposition, collagen and elastin degeneration, and the occurrence of benign or malignant skin tumors (3, 4).

Long-term UV irradiation creates oxidative stress by upregulating reactive oxygen species (ROS) production and simultaneously inhibiting the activity of antioxidant enzymes including SOD and glutathione peroxidase (GSH-Px) (5, 6). Accumulation of ROS activates the mitogen-activated protein kinases (MAPKs) signaling pathway, including c-Jun N-terminal kinase (JNK), p38 MAPK, and extracellular signal-regulated kinase (ERK), which are involved in the regulation of inflammation, cell differentiation, and apoptosis of skin tissue (7). Moreover, ROS degrades collagen by upregulating MMP expression. MMPs are zinc-containing endopeptidases with numerous substrate specificities that degrade a variety of protein substrates, including collagen and elastin, outside the matrix (8). Based on their structure and substrate specificity, MMPs are mainly divided into five categories: collagenases, gelatinases, stromelysins, interstitial lysins, and membrane-type MMPs (9). Phosphorylation of the MAPK signaling pathway subsequently activates downstream transcription factor activator-transforming protein 1 (AP-1), which upregulates protein and gene expression of MMP1, MMP3, and MMP9 to degrade collagen and other extracellular matrix components (10, 11).

Inflammatory factors interleukin 1-beta (IL-1β), IL-6, IL-12, IL-18, and tumor necrosis factor-alpha (TNF-α) are released *via* the NF-κB-TNF-α cascade within UV-photodamaged skin tissue (12, 13). At present, retinoic acid is still the main drug recognized for the clinical treatment of photoaging damage. Intracorporeally, retinoic acid can bind to the corresponding receptors (RAR and RXR) in the body (14) and inhibit phosphorylation of the JNK protein of the MAPKs family, thus preventing the synthesis of downstream transcription factor AP-1 from proto-oncogenes *c-Fos* and *c-Jun*. MMP activity and the NF-κB pathway are simultaneously inhibited, thereby reducing the degradation of collagen and elastin and reducing inflammation in photoaged skin (15).

3′′-*tert*-Butyl-4′-(2-hydroxy-ethoxy)-4′′-pyrrolidin-1-yl-[1,1′,3′,1′′]terphenyl-4-carboxylic acid (trifarotene, Fig. S1) is a functional analogue of retinoic acid. Previous studies revealed that the main mechanisms of action of retinoic acid derivatives are anti-inflammatory, antioxidant, and cause reduction of DNA damage, among others (15, 16). This family of drugs promotes keratogenesis in keratinocytes, fibroblasts, and melanocytes of photoaged skin (17), reducing melanin pigmentation, MMP secretion, and collagen degradation, thereby increasing total skin collagen content (14, 18). However, the application of retinoids is limited due to their association with skin inflammation, epidermal barrier dysfunction, and tolerance in the long term (14). Trifarotene has been shown to function with similar therapeutic efficacy to retinoic acid at half minimal effective concentration, with reduced safety risks even at double the intended market dose (19). In this study, we aimed to investigate trifarotene for its regulation of inflammation, oxidation, and apoptosis in UV-induced photoaging ICR and BALB/c nude (BALB/c-nu) mouse models and in UVB-photoaging HaCaT cell models.

EXPERIMENTAL

ICR mice photoaging model and drug administration

84 ICR mice, 18–22 g, half male, half female, were purchased from Hangzhou Medical College (Hangzhou, Zhejiang, China, license no. SCXK (Zhe) 2019-0002) and housed in an

animal room (ambient temperature 18–24 °C, relative humidity 70 %) with a 12 h light/dark cycle and free access to food and water. All experimental procedures were performed in compliance with the National Institutes of Health (China) guidelines for the care and use of animals and approved by the China Pharmaceutical University Animal Experimental Committee. Based on published studies and preliminary tests, the minimum erythema dose (MED) was determined to be 2760 mJ cm^{-2} for UVA radiation and 280 mJ cm^{-2} for UVB radiation. 14 mice were separated into the blank control group. To establish the photoaging animal model, all ICR mice were anesthetized, and the back skin was depilated (3.5 × 2.5 cm). Two 40W UVA (0.824 mW cm^{-2}) and two UVB (0.037 mW cm^{-2}) lamps were stationed 13 cm above the mice. All mice except those in the blank control were irradiated using 70 % of the MED (1930 mJ cm^{-2} UVA, 196 mJ cm^{-2} UVB) in the first week, and then in increments increasing by 35 % of the MED each week until week 5. The irradiation dose (5790 mJ cm^{-2} UVA, 588 mJ cm^{-2} UVB) was maintained until the 8th week when the photoaging model was successfully constructed, as represented by rough, loose, and deeply wrinkled back skin. In the 9th week, irradiated mice were randomly divided into 5 groups: model control, positive drug (0.02 % retinoic acid, 50 μg per mouse), 0.001 % trifarotene (2.5 μg per mouse), 0.005 % trifarotene (12.5 μg per mouse), and 0.01 % trifarotene (25 μg per mouse), with 14 mice per group. Drug treatment, all in the form of a cream, was applied to the back skin area of all mice in a 0.5 mL dose once per day, 5 days a week for 4 consecutive weeks.

BALB/c nude mice photoaging model and drug administration

84 BALB/c-nu mice, 6–8 weeks old, half male, half female, were purchased from Hangzhou Ziyuan Experimental Animal Technology Co., Ltd (license no. SCXK (zhe) 2019-0004). Animals were housed in the same standard conditions as the ICR mice. All experimental procedures were approved by the China Pharmaceutical University Animal Experimental Committee in compliance with the National Institutes of Health guidelines for the care and use of animals. Nude mice MED was determined to be 1850 mJ cm^{-2} for UVA radiation and 220 mJ cm^{-2} for UVB radiation. 14 mice were set aside as blank control. Two UVA (0.755 mW cm^{-2}) and two UVB (0.027 mW cm^{-2}) lamps were positioned 13 cm above the mice. All mice except the blank control were subjected to 70 % of the MED (1300 mJ cm^{-2} UVA, 150 mJ cm^{-2} UVB) for the first two weeks. From weeks 3–6, UVA irradiation was increased by 35 % MED, and UVB irradiation was increased by 30 mJ cm^{-2} each week. BALB/c-nu mice were subjected to 8 more weeks of UV radiation at the intensity of the 6th week (3900 mJ cm^{-2} UVA, 270 mJ cm^{-2} UVB), wherein the nude mouse skin photoaging model was evaluated according to the criteria in Table I. Simultaneously, mice were randomly divided into 5 groups: model control, positive drug (0.02 % retinoic acid, 50 μg per mouse), 0.001 % trifarotene (2.5 μg per mouse), 0.005 % trifarotene (12.5 μg per mouse), and 0.01 % trifarotene (25 μg per mouse), with 14 mice per group. Drug treatment was applied at the start of the 7th week to the back skin area in a 0.5 mL dose once per day, 5 days a week for 2 weeks.

Skin wrinkle scoring

Upon completion of photoaging and drug administration, the appearance of back skin tissue was evaluated by one researcher according to the standards in Table I below. Blind scoring was completed through the evaluation of all mice's back skin tissue without knowing group identification.

Table I. Photoaging skin wrinkle analysis

Score	Skin representation
0	No wrinkles or sagging; normal fine longitudinal texture
1	Visible fine wrinkles
2	Normal skin texture not visible; many fine wrinkles
3	Visible shallow wrinkles
4	Few deep wrinkles and mild sagging
5	Significant increase in deep wrinkles
6	Severe wrinkles and skin damage

Histochemical staining

For all stains, the skin tissue of 4 mice from each group was fixed in 4 % paraformaldehyde (PFA) for 48 hours, paraffinized, cut into 4 μm sections, and deparaffinized 24 hours after experimentation. For hematoxylin and eosin staining, tissues were stained with HE. For Masson's trichrome, tissues were stained with celestine blue dye for 2 min, hematoxylin for 3 min, and Ponceau red dye for 5 min, washing between each stain. For Van Gieson staining, tissue sections were soaked in glacial acetic acid solution for 2 seconds, stained with Van Gieson dye for 5 min, dehydrated twice with 100 % ethanol, and soaked in xylene for 5 min. All tissues were dehydrated and sealed, then imaged and analyzed under a light microscope. The collagen volume fraction (CVF) in Van Gieson stains, represented by the ratio of collagen-positive blue surface to the total tissue area, was quantified using Image J software (version 1.52v, http://imagej.net).

Enzyme-Linked Immunosorbent Assay (ELISA)

Irradiated skin tissue was dissected and homogenized with pre-cooled PBS in a 1:9 ratio on ice, centrifuged at 3000 rpm for 20 min at 4 °C. SOD and malondialdehyde (MDA) content in the supernatant were determined following the instructions on the ELISA kit (Shanghai Enzyme Biotechnology, China). HaCaT cells were harvested 24 hours after drug treatment. Cell supernatant was collected and analyzed for SOD content as described in the instructions on the ELISA kit.

Immunohistochemistry (IHC) staining of GP100

Endogenous peroxidase activity of 4 μm tissue sections was blocked with PBS solution containing 1 % H_2O_2 for 5 min and antigen repair was completed using a citric acid buffer (0.01 mol L^{-1}, pH 6.0). The sections were blocked with 10 % goat serum for 30 min at room temperature to eliminate non-specific reactions, and incubated with PMEL17/GP100 rabbit anti-mouse polyclonal primary antibody (22e4954, Affinity Biosciences, 1:100, China) overnight in a humidified box at 4 °C. Thereafter, sections were incubated with the secondary antibody at 37 °C for 30 min and stained with chromogenic agent 3,3′-diaminobenzidine hydrochloride (DAB, DAB-2031, Fujian Maixin Company, China) for 3–5 min,

then counterstained with hematoxylin and sealed. Tissue samples were photographed under a microscope in a high-power field of view (200×); 3 consecutive high-power fields of view (400×) were randomly selected from each group and analyzed for positive particle quantity, distinguished by the presence of brown-yellow particles in the cytoplasm and interstitium of cells.

HaCaT cells photoaging model and cell dosing paradigm

HaCaT cells were purchased from the Chinese Academy of Medical Sciences (China). HaCaT cells were cultured in Dulbecco's modified Eagle medium (DMEM) containing 10 % fetal bovine serum (Gibco, USA) in an incubator at 37 °C and 5 % CO_2 levels. Cells were evenly seeded into a 6-well plate with 1×10^6 cells/well, then divided into 6 groups (blank control, model control, retinoic acid treatment (3.3 μmol L^{-1}), and three trifarotene treatment groups (1 μmol L^{-1}, 3.3 μmol L^{-1}, 10 μmol L^{-1}, respectively), and incubated for 24 hours. When cell confluence reached 70–80 %, the old culture medium was discarded and all wells except the blank control group were covered with 1 mL of PBS (Beijing Solarbio Technology, China) and subjected to 75 mJ cm^{-2} UVB irradiation. Following radiation treatment, PBS was discarded and replaced with a new culture medium, and all cells were incubated for 24 hours and then harvested for subsequent assay.

CCK-8 detection of cell viability

HaCaT cells were seeded into a 24-well plate (5×10^5 cells/well) and cultured for 24 hours in an incubator, wherein 200 μL of PBS was added to each well. All cells except those in the blank control group were then exposed to 75 mJ cm^{-2} UVB irradiation and cultured for 24 hours. The Cell Counting Kit-8 (CCK, APEXBIO, K1018, USA) was used to detect cell viability.

Western-blot analysis

Irradiated skin tissue (4 mice per group) was homogenized with RIPA lysis buffer (Beyotime Biotechnology Co, China) containing PMSF and quantified by the BCA Protein Assay Kit (Beijing Applygen Technology Co, China). Proteins were separated by SDS--PAGE and transferred to polyvinylidene fluoride (PVDF) membranes. Membranes were blocked with 5 % skimmed milk for 2 hours, then incubated with MMP1 rabbit anti-mouse polyclonal antibody (00094817, Proteintech Group, 1: 2000, China), MMP3 mouse anti-mouse monoclonal antibody (10004646, Proteintech Group, 1: 5000), and GAPDH mouse anti-mouse monoclonal antibody (10027863, Proteintech Group, 1: 5000) at 4 °C overnight. Membranes were then incubated with HRP-conjugated goat anti-rabbit secondary antibody (56j9958, Affinity Biosciences, 1: 5000, China) and goat anti-mouse secondary antibody (20000242, Proteintech Group, 1: 5000, China) for 2 hours at room temperature. The membranes were visualized under chemiluminescence and analyzed for gray strip value using GADPH as an internal reference.

HaCaT cells were treated as described above. Membranes were incubated overnight with MMP1 rabbit anti-mouse polyclonal antibody (1:2000), MMP3 rabbit anti-mouse polyclonal antibody (AF0217, Affinity Biosciences, 1:2000), and GAPDH mouse anti-mouse

monoclonal antibody (1: 5000) at 4 °C. The membranes were incubated with the secondary antibodies, visualized, and analyzed as described above.

To detect protein expression related to the JNK/c-Jun/MMPs signaling pathway in the HaCaT cell line, HaCaT nuclear and plasma protein were extracted using the nuclear protein and cytoplasmic protein extraction kit (Jiangsu Kaiji Biotechnology Co., Ltd., China), quantified by BCA assay, separated by SDS-PAGE, transferred to PVDF membrane, and incubated with JNK rabbit anti-mouse polyclonal antibody (N10251295, Wanleibio, 1:800, China), phospho-JNK rabbit anti-mouse monoclonal antibody (R03311813, Wanleibio, 1:800), c-Jun rabbit anti-mouse polyclonal antibody (9165T, CST, 1:1000, USA), phospho-c-Jun rabbit anti-mouse polyclonal antibody (3270T, CST, 1:1000), GAPDH mouse anti-mouse monoclonal antibody (1:5000) overnight at 4 °C. The membranes were then incubated with secondary antibodies, visualized, and analyzed as described above.

Statistical analysis

Statistical analysis was performed using IBM SPSS 22.0 statistical software (version 19.0). Comparisons between multiple groups were performed using one-way ANOVA. Fischer's Least Significant Difference (LSD) test was used where experimental data were consistent with the homogeneity of variances, and the Games-Howell test was used otherwise. The values $p < 0.05$ indicate a significant difference. All data were represented as mean ± SEM.

RESULTS AND DISCUSSION

Trifarotene reduces skin wrinkle scores and improves skin tissue morphology in UV-irradiated photoaging mice

Figs. 1a,c revealed that in both ICR and BALB/c-nu mice, the irradiation model group presented significantly more deep wrinkles than the blank control and significantly higher ($p < 0.01$) wrinkles scores than all trifarotene dosage groups and the positive drug (0.02 % retinoic acid) group 4 weeks after drug administration. Skin wrinkle scores in the ICR 12.5 and 25 μg trifarotene groups were significantly lower ($p < 0.05$, $p < 0.01$) than in the positive control group.

HE staining results revealed a significant reduction in blue-stained dermal fibroblasts and a significant increase in inflammatory cells of the irradiation model group as compared to the blank control group (Figs. 1b,d). In the ICR-positive drug group, both dermal fibroblast and inflammatory cell count increased, whereas the BALB/c-nu positive drug group demonstrated dermal fibroblast count and decreased inflammatory cell count. In all mice, fibroblast count increased and inflammatory cell count decreased in the 2.5 and 12.5 μg trifarotene groups when compared to the irradiation model group; the 25 μg trifarotene group showed a significant increase in dermal fibroblasts with continuous inflammatory cell infiltration. Of all treatment groups, the 12.5 μg trifarotene group demonstrated the best therapeutic effect by an increase of fibroblast presence and reduction in inflammatory cell infiltration, seconded by the 25 μg trifarotene group.

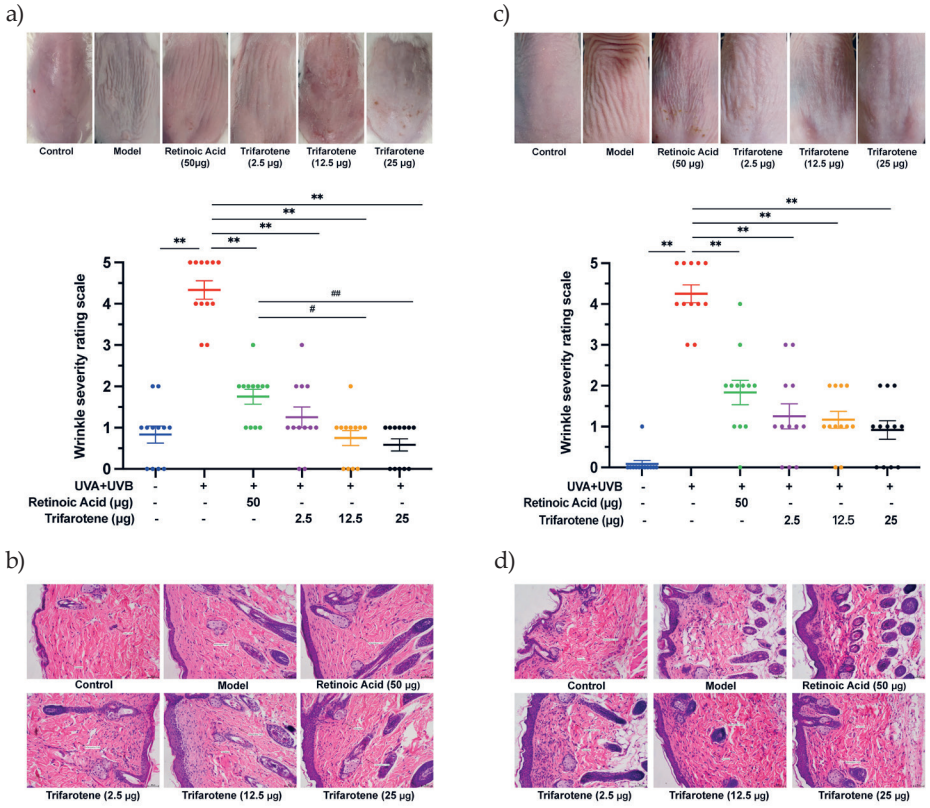

Fig. 1. Trifarotene reduces wrinkle severity and inflammatory cell infiltration in UV-induced photoaging skin. a) Photographs of irradiated ICR mouse skin tissue 4 weeks after treatment (n = 12); b) HE-stained histological images of irradiated ICR mouse tissue 4 weeks after treatment (n = 12, scale bar = 50 μm); c) photographs of irradiated BALB/c-nu mouse skin tissue 2 weeks after treatment (n = 12); d) HE-stained histological images of irradiated BALB/c-nu mouse tissue 2 weeks after treatment (n = 12, scale bar = 50 μm). Data are represented as mean ± SEM in A and C. $^{*}p < 0.05$, $^{**}p < 0.01$ compared to the model control. $^{\#}p < 0.05$, $^{\#\#}p < 0.01$ compared to the positive drug control.

Trifarotene reduces oxidative stress damage and release of inflammatory cytokines in the skin tissue of photoaging mice

UV radiation significantly reduced SOD content and increased MDA content in skin tissue ($p < 0.01$, Fig. 2a, Fig. S2c). All doses of trifarotene and the positive drug control significantly alleviated the effects of irradiation by increasing SOD content ($p < 0.01$); the MDA content in all treatment groups was effectively reduced ($p < 0.01$) except in the ICR 2.5 μg trifarotene group. The positive drug demonstrated a stronger therapeutic effect than all trifarotene dosages in mediating both SOD and MDA content.

UV irradiation caused a significant increase ($p < 0.01$) in the amount of skin tissue inflammatory cytokines IL-6, IL-12, and TNF-α (Fig. 2b, Fig. S2d). All treatment groups

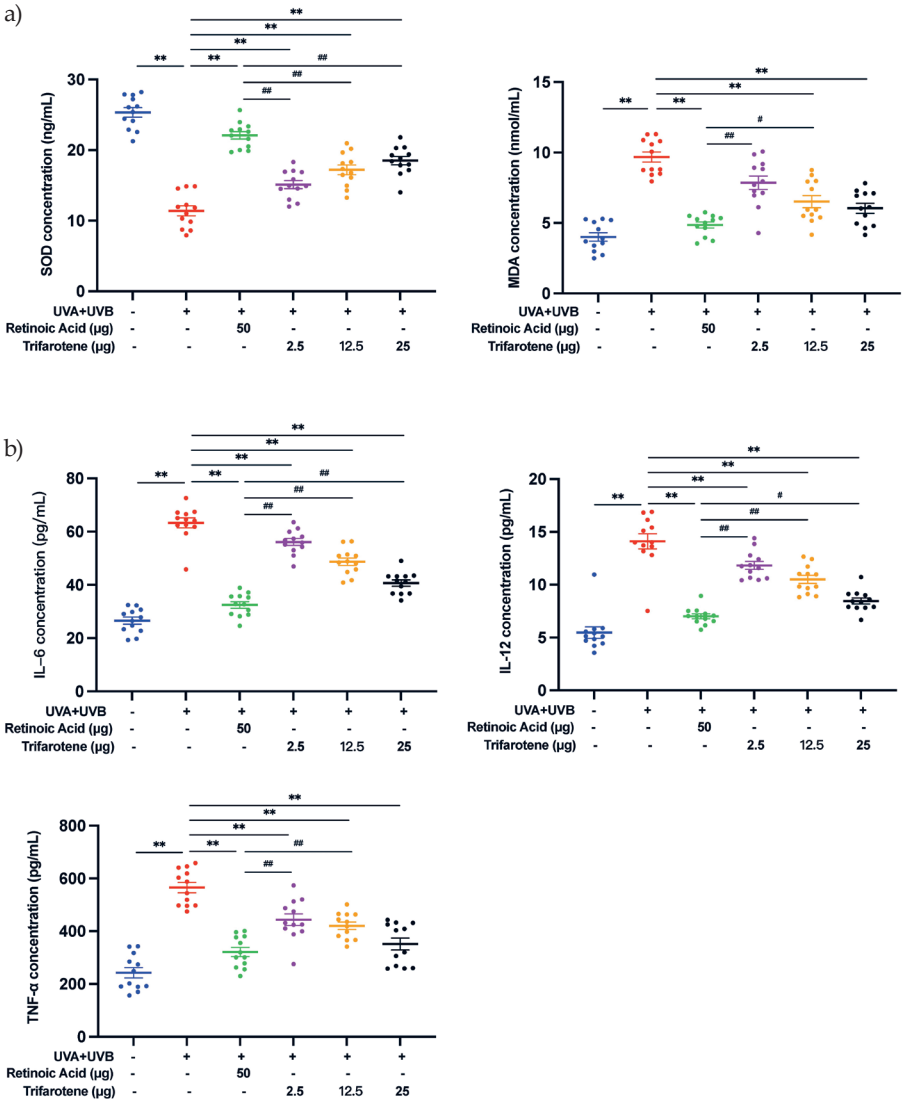

Fig. 2. Trifarotene reduces oxidative stress damage and inhibits inflammatory factor release in photoaging skin. a) SOD and MDA content in irradiated ICR mouse skin tissue (n = 12); b) inflammatory factor concentration in irradiated ICR mouse skin tissue (n = 12). Data are represented as mean ± SEM. $^{*}p < 0.05$, $^{**}p < 0.01$ compared to the model control. $^{\#}p < 0.05$, $^{\#\#}p < 0.01$ compared to the positive drug control.

effectively reduced inflammatory factor content in mouse skin tissue ($p < 0.01$); the positive drug control displayed a significantly stronger effect at lowering inflammatory factor levels than all trifarotene dosages except with the ICR 25 μg trifarotene control group in reducing TNF-α content.

Trifarotene reduces melanin deposition in the skin tissue of photoaging mice

The effects of trifarotene on modulating melanin deposition were assessed by the detection of GP100 and tyrosinase (TyR) expression in photoaging mouse skin. Compared with the blank control group, GP100 expression in the skin of mice in the irradiation model group increased significantly, spreading beyond the surface epithelium to the dermis and hair follicle cells (Figs. 3a,b,d,e). The positive drug group showed an insignificant decrease in GP100 expression and migration of cells from the model group. GP100-expression in all trifarotene groups significantly decreased from the irradiation model group ($p < 0.01$) and positive drug group ($p < 0.01$) and was concentrated focally in the dermis.

TyR content in the skin tissue of mice in the irradiation model group significantly increased ($p < 0.01$) from that of the blank control (Fig. 3c,f); TyR content in all trifarotene groups was significantly lower ($p < 0.01$) than that of the model group, and the positive drug group demonstrated further reduction than all trifarotene groups ($p < 0.01$).

Trifarotene increases dermal collagen content in the skin tissue of photoaging mice

To investigate how trifarotene increases collagen content in photoaging skin tissue, dermal collagen arrangement and collagen volume fraction (CVF) were assessed by Masson's Trichrome and Van Gieson staining. Irradiation model group dermal collagen tissue was comparatively disordered with homogenous degeneration and significantly reduced ($p < 0.01$) CVF against the blank control group (Fig. S3a-c,e-g). Compared with the model group, collagen tissue of the positive drug group was disordered and homogenously degenerated with no significant change to the CVF in ICR mice and a significant increase ($p < 0.05$) in the CVF of BALB/c-nu mice. In the 2.5 μg trifarotene group, collagen tissue was also disordered and loose, but with significantly increased ($p < 0.05$) CVF in ICR mice and non--significantly increased CVF in BALB/c-nu mice. We observed the best therapeutic effect in the 12.5 μg trifarotene group, characterized by orderly arranged fibers parallel to the epidermis, improved homogenous degeneration, and a significant increase ($p < 0.01$) in the CVF. In the BALB/c-nu 25 μg trifarotene group, mouse skin tissue also demonstrated significantly increased ($p < 0.01$) CVF, with no other improvements.

This study also measured HyP content, a major component of protein collagen, in photoaging skin tissue as an indicator of collagen content. Model control tissue subjected only to irradiation possessed significantly lower ($p < 0.01$) HyP content than the blank control, and HyP content was alleviated in all treatment groups ($p < 0.01$, Fig. S3d,h). The ICR 2.5 and 12.5 μg trifarotene groups and all BALB/c-nu trifarotene groups demonstrated significantly lower therapeutic effects compared to retinoic acid.

Trifarotene inhibits protein expression of MMPs in photoaging mouse skin tissue

The expression of two major MMPs involved in collagen degradation, MMP1 and MMP3, were evaluated by Western blot. As presented in Fig. 4, exposure to UV radiation without treatment significantly increased the expression of MMP1 and MMP3. Administration of the positive drug control and all doses of trifarotene significantly reduced MMP1 and MMP3 expression compared to the irradiation model group.

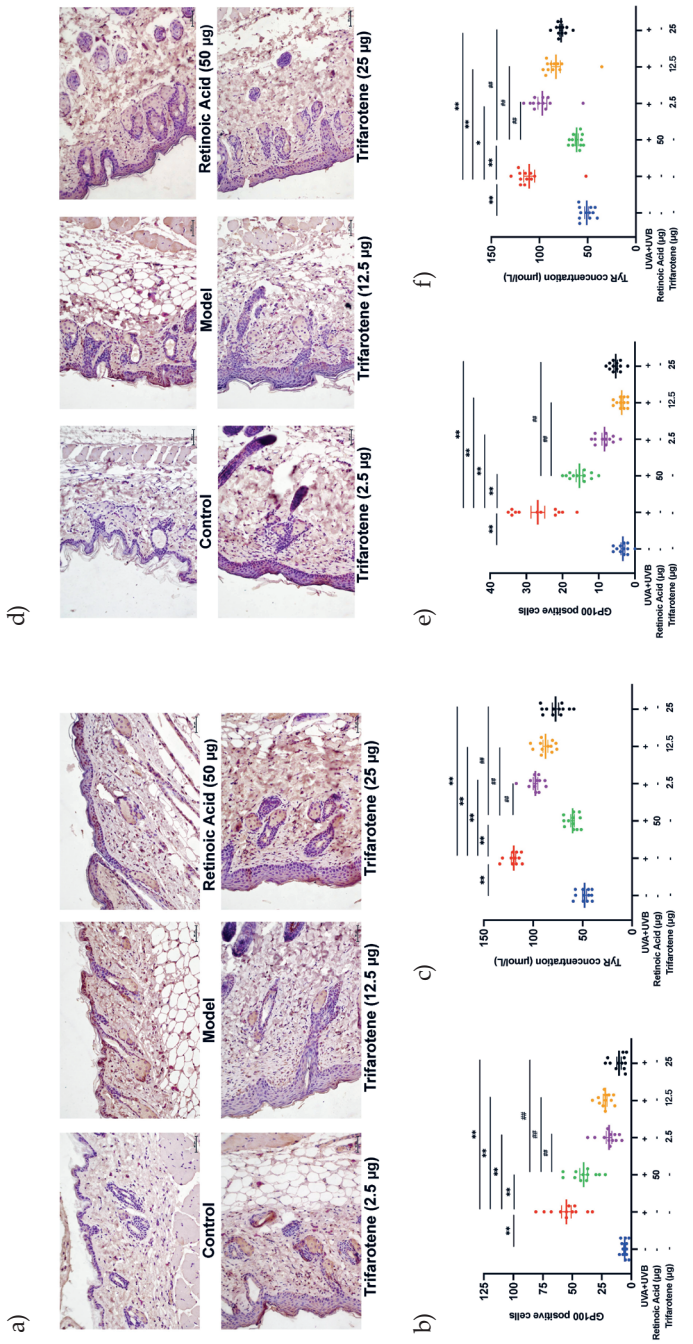

Fig. 3. Trifarotene reduced GP100 and TyR expression in photoaging mouse skin. a) and b) GP100 expression and quantification in photoaging ICR mouse skin tissue (n = 12, scale bar = 50 μm); c) TyR concentration in photoaging ICR mouse skin tissue (n = 12); d-e) GP100 expression and quantification in photoaging BALB/c-nu mouse skin tissue (n = 12, scale bar = 50 μm); f) TyR concentration in photoaging BALB/c-nu mouse skin tissue (n = 12). Data are represented as mean ± SEM in figures b, c, e, and f. $^{*}p < 0.05$, $^{**}p < 0.01$ compared to the model control. $^{\#}p < 0.05$, $^{\#\#}p < 0.01$ compared to the positive drug control.

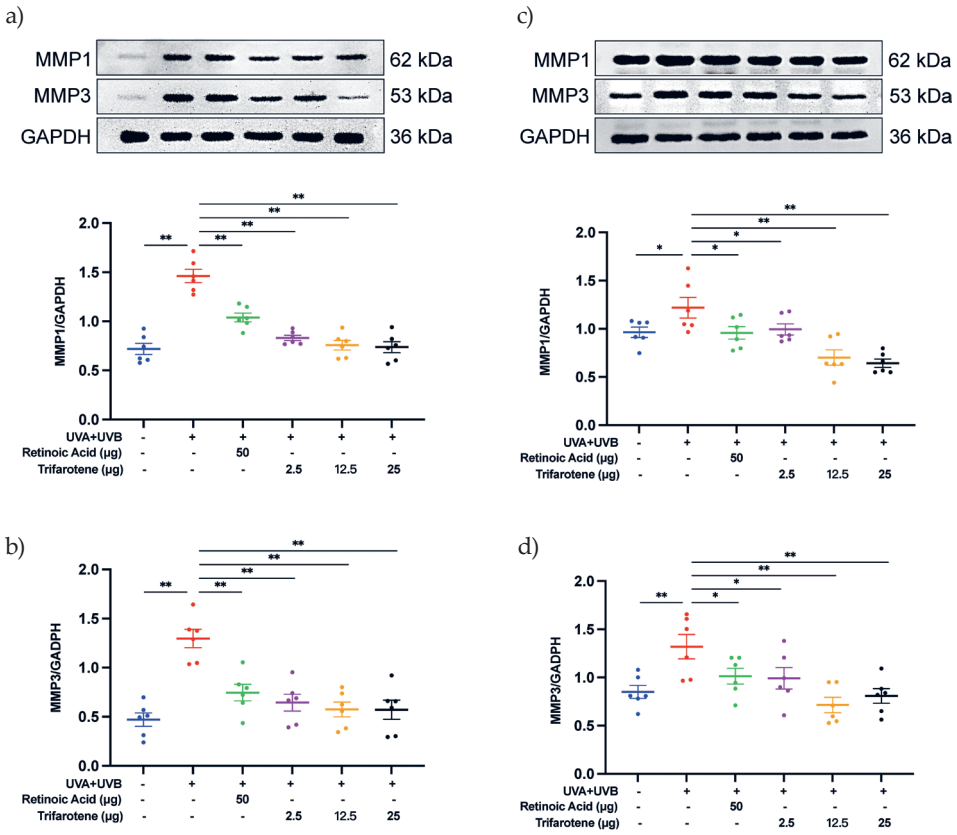

Fig. 4. Trifarotene reduces MMP1 and MMP3 expression in UV-irradiated mouse skin tissue. a) and b) Representative Western blot images and quantification of MMP1 and MMP3 expression in irradiated ICR mice ($n = 6$); c) and d) representative Western blot images and quantification of MMP1 and MMP3 expression in irradiated BALB/c-nu mice ($n = 6$). Data are represented as mean ± SEM. *$p < 0.05$, **$p < 0.01$ compared to the model control.

Trifarotene increases cell viability and supernatant SOD content and inhibits MMP expression in photoaging HaCaT cells

HaCaT cells subjected to 75 mJ cm^{-2} of UVB irradiation experienced a significant reduction ($p < 0.01$) in cell proliferation and SOD content in the cell supernatant (Fig. S4a,b), an effect that was mitigated by all trifarotene (1, 3.3 and 10 μmol L^{-1}) groups.

Figs. S4c,d revealed a significant increase ($p < 0.01$) in HaCaT MMP1 and MMP3 expression in the irradiation model group compared to the blank control. All treatment groups significantly reduced MMP1 expression, and all but the 1 μmol L^{-1} trifarotene dosage group significantly reduced MMP3 expression.

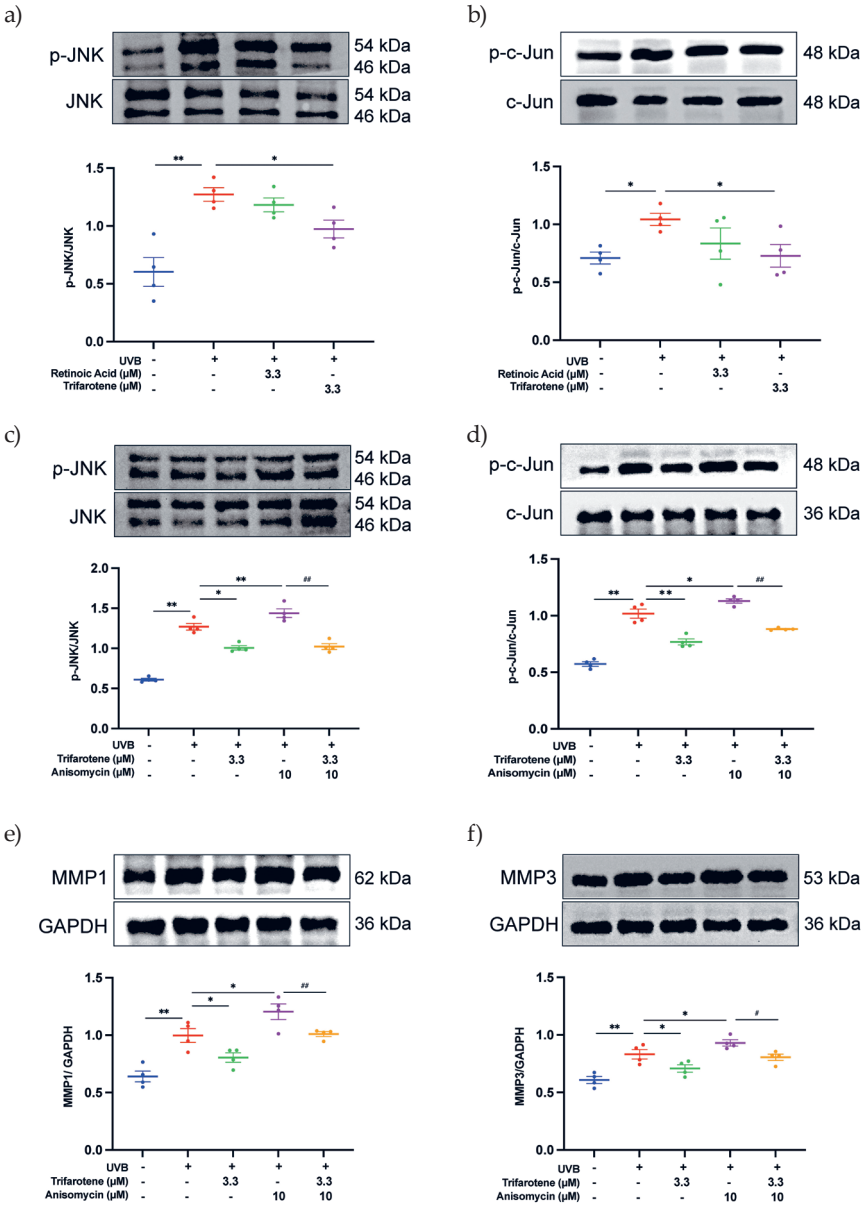

Fig. 5. Trifarotene downregulates protein expression of the JNK/c-Jun/MMPs signaling pathway in photoaging HaCaT cells. a) and b) Representative Western blot images and quantification of phosphorylated JNK and phosphorylated c-Jun compared to the positive drug ($n = 4$); c) to f) representative Western blot images and quantification of phosphorylated JNK, phosphorylated c-Jun, MMP1, and MMP3 ($n = 4$). Data are represented as mean ± SEM. $^{*}p < 0.05$, $^{**}p < 0.01$ compared to the model control. $^{\#}p < 0.05$, $^{\#\#}p < 0.01$ compared to anisomycin.

Trifarotene down-regulates the expression of JNK/c-Jun/MMPs signaling pathway-related proteins in photodamaged HaCaT cells

As shown in Fig. 5a,b, UV irradiation significantly increased the expression of phosphorylated JNK ($p < 0.01$) and phosphorylated c-Jun ($p < 0.05$) proteins in HaCaT cells. Trifarotene (3.3 μmol L^{-1}) was able to significantly reduce ($p < 0.05$) expression of both phosphorylated proteins. Fig. 5c-f reveals that the protein expression of phosphorylated JNK, c-Jun, MMP1, and MMP3 in the JNK activator (Anisomycin) group was all significantly increased when compared with the irradiation model groups. However, the combination of trifarotene (3.3 μmol L^{-1}) with the JNK activator significantly reduced all protein expression levels compared to that of the JNK activator alone.

Therapeutic effects and mechanisms of trifarotene

Our results showed that trifarotene effectively reduced phenotypical manifestations of skin photoaging by enhancing dermal collagen content and arrangement as measured by CVF and HyP content. It also performed antioxidant and anti-inflammatory functions, increasing SOD content and reducing expression of inflammatory factors IL-6, IL-12, and TNF-α. Trifarotene decreased melanin deposition as demonstrated through lowered GP100 and TyR expression, and alleviated collagen degradation through anti-MMP action. This study found that trifarotene functioned equivalently to the positive drug at half the minimal effective concentration, indicating great potential as a therapeutic for UV-induced skin photoaging with reduced risk of inflammatory and allergic side effects.

Ultraviolet radiation is categorized into UVA (320–400 nm), UVB (280–320 nm), and UVC (200–280 nm), of which UVC is absorbed and scattered by the ozone layer (20). UVA has a high penetrative ability and stimulates dermal fibroblasts and vascular endothelial cells to promote the expression of MMPs, which catalyze the degradation of collagen and elastin, thereby changing the dermal structure and causing skin sagging (21, 22). UVA irradiation also stimulates melanosomes, whereby continued production of melanin leads to melanin deposition and darkening of the skin (23). This study investigates the therapeutic effects of trifarotene against photoaging, including excess melanin deposition as a key clinical manifestation. Reduction in melanin deposition is therefore considered an alleviating process of damage caused under an experimental UV-induced photoaging condition. UVB radiation is mostly absorbed by the epidermis, where it causes lesions, thickening of the stratum corneum, aggravation of the inflammatory response (21), and the release of a variety of chemical mediators that cause local blood vessel dilation, commonly manifested as erythema on the skin (24). When working concurrently, UVA induces peroxidation, causes secondary damage, and enhances the erythema-causing effect of UVB (25).

UVA generates cellular free radicals and lipid peroxides and induces cells in the dermis and subcutaneous tissue, including fibroblasts, vascular endothelial cells, and Langerhans cells to express MMPs (26). Both the accumulation of ROS and MMPs, of which MMP1 and MMP3 are key factors in the photoaging process (5), catalyze the degradation of collagen and elastin and cause changes in the dermal structure, leading to skin sagging and an abnormal increase in skin wrinkles. Van Gieson and Masson staining was used to evaluate dermal collagen and fibroblast content. Trifarotene demonstrated a therapeutic

effect in improving collagen volume fraction and arrangement and increasing HyP content in UV-irradiated photoaging mouse models.

Western blot detection of MMP1 and MMP3 revealed that trifarotene at all dosages significantly inhibited MMP1 and MMP3 protein expression in photoaging ICR and BALB/c-nu mouse models; in the HaCaT photoaging cell line, trifarotene (3.3 μmol L^{-1}) significantly reduced MMP1 and MMP3 expression (Fig. 4, Fig. S4e-f). These results signify that trifarotene at concentrations ranging from 2.5 to 25 μg is effective in preventing UV-induced MMP proliferation and collagen degradation in both *in vivo* and *in vitro* photoaging models.

Skin keratinocytes secrete a variety of antioxidant enzymes including SOD, catalase (CAT), and glutathione peroxidase (GSH-Px) to remove ROS and maintain cellular redox (27). Under UVB irradiation, secretion of antioxidant enzymes, inflammatory factors, and other chemical mediators are spread to the dermis (28); concurrent UVB inhibition of antioxidant activity results in the accumulation of ROS, thereby exacerbating the inflammatory reaction and causing oxidative stress (29, 30). In this study, we used ELISA to detect the levels of oxidoreductase SOD and MDA, inflammatory factors IL-6, IL-12, and TNF-α, and the levels of TyR. The results showed that trifarotene mitigated the oxidative effects of photoaging by significantly increasing SOD content and decreasing MDA content (Fig. 2a), Fig. S2c). Trifarotene (1, 3.3, and 10 μmol L^{-1}) significantly increased SOD content and reduced oxidative stress damage in HaCaT cells, and trifarotene at concentrations of 1 and 3.3 μmol L^{-1} was more effective than retinoic acid in reducing oxidative stress damage.

Basal melanocytes of the epidermis use tyrosinase to catalyze tyrosine to produce dopa, which is oxidized multiple times to produce melanin (31, 32). TyR is often used to evaluate melanin production because it is a key enzyme for melanin production in the body (33, 34). Our results demonstrated that trifarotene effectively reduced levels of inflammatory factors IL-6, IL-12, and TNF-α, as well as TyR and GP100 expression count in both in-vivo photoaging mouse models (Fig. 2b, Fig. S2d, Fig. 3).

HaCaT cells are immortalized keratinocytes and are extensively used in the study of skin barrier abnormalities and dermatological diseases (35). Inflammatory and MMP signaling typically targets dermal cells but also triggers HaCaT cells to release secondary inflammatory mediators and degrade collagen through ROS-dependent signaling cascades (36). ROS accumulation induces the phosphorylation of the MAPKs family (5), activating kinases such as ERK, p38, and JNK, and subsequently triggering the downstream *c-Fos* and *c-Jun* to synthesize the transcription factor Activator protein 1 (AP-1) (21, 37, 38). This pathway promotes the secretion of MMPs, thereby promoting the degradation of collagen fibers and inducing skin photoaging (30, 39, 40). This study used Western blot to detect the expression of proteins related to the JNK/c-Jun/MMPs pathway in HaCaT photodamaged cells. The results showed that trifarotene (3.3 μmol L^{-1}) may mediate UV-induced photoaging by significantly reducing the expression of MMP1, MMP3, phosphorylated c-Jun, and phosphorylated JNK proteins.

Although promising for the treatment of UV-induced skin aging, the use of trifarotene for photoaging is likely to coincide with the treatment of acne vulgaris: retinoids are commonly prescribed for acne medication but face impediment by common irritation of the skin (41). Trifarotene (0.005 %) as an acne treatment has been shown to cause irritation during short-term application (41). More research is required on the interplay between the effects of trifarotene on UV-induced photoaging and acne vulgaris, along with the effects of long-term trifarotene use on the skin.

CONCLUSIONS

Trifarotene demonstrated therapeutic effect against UV-induced photoaging by inhibiting MMP expression and reducing collagen degradation, alleviating oxidative stress by balancing SOD expression, and limiting the inflammatory response by lowering phosphorylated JNK and c-Jun kinases of the MAPK pathway in ICR and BALB/c-nu mice and the HaCaT cell line. These results present trifarotene as a promising therapeutic alternative against retinoic acid, achieving the same therapeutic effect at a lower minimum effective dose while curbing the common allergic and inflammatory complications of retinoic acid. However, future studies on the underlying mechanisms, safety evaluation, and potential side effects of trifarotene as a therapeutic on photoaged skin are still needed.

Institutional review board statement. – The study was conducted in accordance with the Declaration of Helsinki, and approved by the Ethics Committee of China Pharmaceutical University (approval number: 2022-04-020)

Data availability. – All datasets are available from the corresponding author upon reasonable request.

Conflict of interest. – The authors declare no conflict of interest.

Funding. – This research received no external funding.

Authors contributions. – Conceptualization, X.F. and W.F.; methodology, X.F.; analysis, L.Z.Y.; investigation, X.F., J.Z., X.L., M.P. and G.X.; writing, original draft preparation, L.Z.Y.; writing, review and editing, L.Z.Y. and W.F.; visualization, X.F. and L.Z.Y.; resources, C.Z. and F.L. All authors have read and agreed to the published version of the manuscript.

REFERENCES

1. L. Rittie and G. J. Fisher, Natural and sun-induced aging of human skin, *Cold Spring Harb. Perspect. Med.* **5**(1) (2015) Article ID a015370 (15 pages); https://doi.org/10.1101/cshperspect.a0 15370
2. W. Gao, Y.-S. Wang, E. Hwang, P. Lin, J. Bae, S. A. Seo, Z. Yan and T.-H. Yi, *Rubus idaeus* L. (red raspberry) blocks UVB-induced MMP production and promotes type I procollagen synthesis via inhibition of MAPK/AP-1, NF-kappabeta and stimulation of TGF-beta/Smad, Nrf2 in normal human dermal fibroblasts, *J. Photochem. Photobiol.* B. **185** (2018) 241–253; https://doi.org/10.1016/j.jphotobiol.2018.06.007
3. M. Wlaschek, I. Tantcheva-Poor, L. Naderi, W. Ma, L. A. Schneider, Z. Razi-Wolf, J. Schüller and K. Scharffetter-Kochaneck, Solar UV irradiation and dermal photoaging, *J. Photochem. Photobiol.* B. **63**(1–3) (2001) 41–51; https://doi.org/10.1016/s1011-1344(01)00201-9
4. Y. Gu, J. Han, C. Jiang and Y. Zhang, Biomarkers, oxidative stress and autophagy in skin aging, *Ageing Res. Rev.* **59** (2020) Article ID 101036 (12 pages); https://doi.org/10.1016/j.arr.2020.101036
5. E. Fitsiou, T. Pulido, J. Campisi, F. Alimirah and M. Demaria, Cellular senescence and the senescence-associated secretory phenotype as drivers of skin photoaging, *J. Invest. Dermatol.* **141**(4S) (2021) 1119–1126; https://doi.org/10.1016/j.jid.2020.09.031
6. G. Petruk, R. Del Giudice, M. M. Rigano and D. M. Monti, Antioxidants from plants protect against skin photoaging, *Oxid. Med. Cell Longev.* **2018** (2018) Article ID 1454936 (11 pages); https://doi.org/10.1155/2018/1454936
7. J. H. Oh, F. Karadeniz, J. I. Lee, S. Y. Park, Y. Seo and C. S. Kong, Anticatabolic and anti-inflammatory effects of myricetin 3-*O*-beta-D-galactopyranoside in UVA-irradiated dermal cells via repression of MAPK/AP-1 and activation of TGFbeta/Smad, *Molecules* **25**(6) (2020) e1331 (18 pages); https://doi.org/10.3390/molecules25061331

8. N. Xue, Y. Liu, J. Jin, M. Ji and X. Chen, Chlorogenic acid prevents UVA-induced skin photoaging through regulating collagen metabolism and apoptosis in human dermal fibroblasts, *Int. J. Mol. Sci.* **23**(13) (2022) e6941 (14 pages); https://doi.org/10.3390/ ijms23136941
9. P. Pittayapruek, J. Meephansan, O. Prapapan, M. Komine and M. Ohtsuki, Role of matrix metalloproteinases in photoaging and photocarcinogenesis, *Int. J. Mol. Sci.* **17**(6) (2016) e868 (20 pages); https://doi.org/10.3390/ijms17060868
10. H.-S. Han, J.-S. Shin, D.-B. Myung, H. S. Ahn, S. H. Lee, H. J. Kim and K.-T. Lee, *Hydrangea serrata* (Thunb.) ser. extract attenuate UVB-induced photoaging through MAPK/AP-1 inactivation in human skin fibroblasts and hairless mice, *Nutrients* **11**(3) (2019) e533 (15 pages); https://doi.org/10.3390/nu11030533
11. P. V. Kandan, A. Balupillai, G. Kanimozhi, H. A. Khan, A. S. Alhomida and N. R. Prasad, Opuntiol prevents photoaging of mouse skin via blocking inflammatory responses and collagen degradation, *Oxid. Med. Cell Longev.* **2020** (2020) Article ID 5275178 (20 pages); https://doi.org/10.1155/2020/5275178
12. T. M. Ansary, M. R. Hossain, K. Kamiya, M. Komine and M. Ohtsuki, Inflammatory molecules associated with ultraviolet radiation-mediated skin agin *Int. J. Mol Sci.* **22**(8) (2021) e3874 (14 pages); https://doi.org/10.3390/ijms22083974
13. M. Burian and A. S. Yazdi, NLRP1 Is the key inflammasome in primary human keratinocytes, *J. Invest. Dermatol.* **138**(12) (2018) 2507–2510; https://doi.org/10.1016/j.jid.2018.08.004
14. L. Szymanski, R. Skopek, M. Palusinska, T. Schenk, S. Stengel, S. Lewicki, L. Kraj, P. Kamiński and A. Zelent, Retinoic acid and its derivatives in skin, *Cells* **9**(12) (2020) e2660 (14 pages); https://doi.org/10.3390/cells9122660
15. R. R. Riahi, A. E. Bush and P. R. Cohen, Topical retinoids: Therapeutic mechanisms in the treatment of photodamaged skin, *Am. J. Clin. Dermatol.* **17**(3) (2016) 265–276; https://doi.org/10.1007/s40257-016-0185-5
16. A. J. Stratigos and A. D. Katsambas, The role of topical retinoids in the treatment of photoaging, *Drugs* **65**(8) (2005) 1061–1072; https://doi.org/10.2165/00003495-200565080-00003
17. A. Ascenso, H. Ribeiro, H. C. Marques, H. Oliveira, C. Santos and S. Simoes, Is tretinoin still a key agent for photoaging management?, *Mini Rev. Med. Chem.* **14**(8) (2014) 629–641; https://doi.org/10.2174/1389557514666140820102735
18. D. Milosheska and R. Roskar, Use of retinoids in topical antiaging treatments: A focused review of clinical evidence for conventional and nanoformulations, *Adv. Ther.* **39**(12) (2022) 5351–5375; https://doi.org/10.1007/s12325-022-02319-7
19. N. Wagner, K. Benkali, A. A. Sáenz, M. Poncet and M. Graeber, Clinical pharmacology and safety of trifarotene, a first-in-class RARγ-selective topical retinoid, *J. Clin. Pharmacol.* **60**(5) (2020) 660–668; https://doi.org/10.1002/jcph.1566.
20. Y. Matsumura and H. N. Ananthaswamy, Toxic effects of ultraviolet radiation on the skin, *Toxicol. Appl. Pharmacol.* **195**(3) (2004) 298–308; https://doi.org/10.1016/j.taap.2003. 08.019
21. M. Sawane and K. Kajiya, Ultraviolet light-induced changes of lymphatic and blood vasculature in skin and their molecular mechanisms, *Exp. Dermatol.* **21**(Suppl 1) (2012) 22–25; https://doi.org/10.1111/j.1600-0625.2012.01498.x
22. C. E. Lan, Y. T. Hung, A. H. Fang and W. Ching-Shuang, Effects of irradiance on UVA-induced skin aging, *J. Dermatol. Sci.* **94**(1) (2019) 220–228; https://doi.org/10.1016/ j.jdermsci.2019.03.005
23. J. Y. Lin and D. E. Fisher, Melanocyte biology and skin pigmentation, *Nature* **445**(7130) (2007) 843–850; https://doi.org/10.1038/nature05660
24. S. H. Hu, S. Jiang, F. Miao and T. C. Lei, sPmel17 Secreted by ultraviolet B-exposed melanocytes alters the intercellular adhesion of keratinocytes, *Oxid. Med. Cell Longev.* **2022** (2022) Article ID 1856830 (12 pages); https://doi.org/10.1155/2022/1856830

25. X. Chen, C. Yang and G. Jiang, Research progress on skin photoaging and oxidative stress, *Postepy Dermatol. Alergol.* **38**(6) (2021) 931–936; https://doi.org/10.5114/ada.2021. 112275

26. M. Wang, P. Charareh, X. Lei and J. L. Zhong, Autophagy: Multiple mechanisms to protect skin from ultraviolet radiation-driven photoaging, *Oxid. Med. Cell Longev.* **2019** (2019) Article ID 8135985 (14 pages); https://doi.org/10.1155/2019/8135985

27. S. Kawashima, T. Funakoshi, Y. Sato, N. Saito, H. Ohsawa, K. Kurita, K. Nagata, M. Yoshida and A. Ishigami, Protective effect of pre- and post-vitamin C treatments on UVB-irradiation-induced skin damage, *Sci. Rep.* **8**(1) (2018) Article ID 16199 (12 pages); https://doi.org/10.1038/s41598-018-34530-4

28. K. Vats, O. Kruglov, A. Mizes, S. N. Samovich, A. A. Amoscato, V. A. Tyurin, Y. Y. Tyurina, V. E. Kagan and Y. L. Bunimovich, Keratinocyte death by ferroptosis initiates skin inflammation after UVB exposure, *Redox Biol.* **47** (2021) Article ID 102143 (12 pages); https://doi.org/10.1016/j.redox.2021.102143

29. T. Xiao, Y. Chen, C. Song, S. Xu, S. Lin, M. Li, X. Chen and H. Gu, Possible treatment for UVB-induced skin injury: Anti-inflammatory and cytoprotective role of metformin in UVB-irradiated keratinocytes, *J. Dermatol Sci.* **102**(1) (2021) 25–35; https://doi.org/10. 1016/j.jdermsci.2021.02.002

30. M. Hatakeyama, A. Fukunaga, K. Washio, K. Taguchi, Y. Oda, K. Ogura and C. Nishigori, Anti-inflammatory role of Langerhans cells and apoptotic keratinocytes in ultraviolet-B-induced cutaneous inflammation, *J. Immunol.* **199**(8) (2017) 2937–2947; https://doi.org /10.4049/jimmunol.1601681

31. S. Hu, J. Huang, S. Pei, Y. Ouyang, Y. Ding, L. Jiang, J. Lu, L. Kang, L. Huang, H. Xiang, R. Xiao, Q. Zeng and J. Chen, Ganoderma lucidum polysaccharide inhibits UVB-induced melanogenesis by antagonizing cAMP/PKA and ROS/MAPK signaling pathways, *J. Cell Physiol.* **234**(5) (2019) 7330–7740; https://doi.org/10.1002/jcp.27492

32. S. A. D'Mello, G. J. Finlay, B. C. Baguley and M. E. Askarian-Amiri, Signaling pathways in melanogenesis, *Int. J. Mol. Sci.* **17**(7) (2016) e1144 (18 pages); https://doi.org/10.3390/ ijms17071144

33. Q. M. Hu, W. J. Yi, M. Y. Su, S. Jiang, S. Z. Xu and T. C. Lei, Induction of retinal-dependent calcium influx in human melanocytes by UVA or UVB radiation contributes to the stimulation of melanosome transfer, *Cell Prolif.* **50**(6) (2017) e12372 (10 pages); https://doi.org/10.1111/cpr.12372

34. Y. J. Liu, J. L. Lyu, Y. H. Kuo, C. Y. Chiu, K. C. Wen and H. M. Chiang, The anti-melanogenesis effect of 3,4-dihydroxybenzalacetone through downregulation of melanosome maturation and transportation in B16F10 and human epidermal melanocytes, *Int. J. Mol. Sci.* **22**(6) (2021) e2823 (15 pages); https://doi.org/10.3390/ ijms22062823

35. M. D. Seo, T. J. Kang, C. H. Lee, A. Y. Lee and M. Noh, HaCaT keratinocytes and primary epidermal keratinocytes have different transcriptional profiles of cornified envelope-associated genes to t helper cell cytokines, *BioMol. Ther.* (Seoul) **20**(2) (2012) 171–176; https://doi.org/10.4062/biomolther.2012.20.2.171

36. C. Kim, H. C. Ryu and J. H. Kim, Low-dose UVB irradiation stimulates matrix metalloproteinase-1 expression via a BLT2-linked pathway in HaCaT cells, *Exp. Mol. Med.* **42**(12) (2010) 833–841; https://doi.org/10.3858/emm.2010.42.12.086

37. M. Jevtic, A. Lowa, A. Novackova, A. Kovacik, S. Kaessmeyer, G. Erdmann, K. Vavrova and S. Hedtrich, Impact of intercellular crosstalk between epidermal keratinocytes and dermal fibroblasts on skin homeostasis, *Biochim. Biophys. Acta Mol. Cell Res.* **1867**(8) (2020) Article ID 118722 (10 pages); https://doi.org/10.1016/j.bbamcr.2020.118722

38. J. H. Oh, Y. H. Joo, F. Karadeniz, J. Ko and C. S. Kong, Syringaresinol inhibits UVA-induced MMP-1 expression by suppression of MAPK/AP-1 signaling in HaCaT keratinocytes and human dermal fibroblasts, *Int. J. Mol. Sci.* **21**(11) (2020) e3981 (12 pages); https://doi.org/10.3390/ijms21113981

39. N. Zhang, Y. Zhao, Y. Shi, R. Chen, X. Fu and Y. Zhao, Polypeptides extracted from Eupolyphaga sinensis walker via enzymic digestion alleviate UV radiation-induced skin photoaging, *Biomed. Pharmacother.* **112** (2019) Article ID 108636 (7 pages); https://doi.org/10.1016/j.biopha.2019.108636
40. Y.-C. Hseu, Y. V. Gowrisankar, L.-W. Wang, Y.-Z. Zhang, X.-Z. Chen, P.-J. Huang, H.-R. Yen. H.-L. Yang, The in vitro and in vivo depigmenting activity of pterostilbene through induction of autophagy in melanocytes and inhibition of UVA-irradiated alpha-MSH in keratinocytes via Nrf2-mediated antioxidant pathways, *Redox Biol.* **44** (2021) Article ID 102007 (17 pages); https://doi.org/10.1016/j.redox.2021.102007
41. Z. D. Draelos, Low irritation potential of tazarotene 0.045% lotion: Head-to-head comparison to adapalene 0.3% gel and trifarotene 0.005% cream in two studies, *J. Dermatol. Treatment* **34**(1) (2023) Article ID 2166346 (7 pages); https://doi.org/10.1080/09546634.2023.2166346